Photochemical and Photophysical Properties of C_{60} Dendrimers Studied by Laser Flash Photolysis

Ryouta Kunieda,[‡] Mamoru Fujitsuka,[‡] Osamu Ito,*[,‡] Miho Ito,[†] Yasujiro Murata,[†] and Koichi Komatsu*[,†]

Institute of Multidisciplinary Research for Advanced Materials, Tohoku University, Katahira, Aoba-ku, Sendai, 980-8577, Japan and Institute for Chemical Research, Kyoto University, Uji, Kyoto 611-0011, Japan

Received: February 27, 2002; In Final Form: May 24, 2002

Photochemical and photophysical properties of fullerene dendrimers, in which the fullerene-moiety was connected via an acetylene bond with benzyl-ether type dendrons from the second to fourth generation, have been investigated by time-resolved fluorescence and time-resolved absorption methods, in addition to steady-state spectra. The photophysical properties of the dendrimers such as lifetimes of the singlet and triplet excited states were essentially the same, regardless of the dendrimer generation. However, the rate constants of intermolecular processes such as triplet−triplet annihilation, triplet energy transfer, and electron transfer via the triplet states decreased with the increase in dendrimer generation. The relation between the free energy changes and the quenching rate constants revealed long-range electron transfer processes due to steric hindrance of the dendron groups. Furthermore, it was revealed that the solvation of radical ion pairs is also affected by size of the dendron groups. Back electron transfer kinetics became first-order for the electron transfer system of the smaller donor and/or smaller dendron groups, while second-order kinetics was observed for larger donor and/or larger dendron groups. The dendron groups were also found to be effective to keep unstable species such as the chemically generated fullerenyl anion persistent.

Introduction

Fullerene-based derivatives have been attracting a great interest in the field of structural and synthetic organic chemistry.[1] In particular, there have been several studies on syntheses and properties of fullerene-functionalized dendrimers, called fullerodendrimers,[2] in which fullerene is incorporated as a core, in branches, or as terminals, because of a variety of interesting features in the field of supramolecular chemistry and material science.[2−18] Introduction of dendritic branches to the fullerene core can improve solubility and processability. Furthermore, it also provides an additional functionality of the branches themselves.[12,13] The possible electronic and steric interaction between the branches and the fullerene core may be interesting as reported for the supramolecular complexes of dendrimers and pristine C_{60}.[15−17] Although a number of fullerodendrimers have been synthesized, studies on their photophysical properties are limited.[7,11,14] The photochemical bimolecular processes of fullerodendrimers such as photoinduced electron transfer have not been disclosed, to our knowledge. In fullerodendrimers having the fullerene moiety as a core, the steric effect of the surrounding dendron group will operate so that the fullerene moieties are separated from each other. This feature is advantageous in application of fullerodendrimers to the devices in the film and solid state, because aggregation of fullerenes which causes fast deactivation of the excited states will become neglected.[18−20] Thus, the clarification of the photophysical properties of fullerodendrimers with various dendrimer generations is important in an attempt for application of these fullerodendrimers to functional materials such as photoactive devices. Furthermore, by introduction of the flexible dendron groups, dynamic characters of the fullerene moiety such as photoinduced reactions can be also controlled. The presence of bulky dendron groups is also expected to make an unstable species persistent by steric protection.

In the present study, fullerene (C_{60}) was connected with benzyl-ether type dendrons as building blocks via the acetylene group as shown in Scheme 1. Schematically, the fullerodendrimers have a conical shape in which the fullerene core exists as a pivot of the fans with second generation (C_{60}G2), third generation (C_{60}G3), and fourth generation (C_{60}G4) dendrons. The photophysical and photochemical properties have been estimated with time-resolved laser techniques to obtain the information as to the bimolecular dynamics of the excited states to disclose the effects of dendrimer moieties in solution.

Experimental Section

Chemicals. Fullerodendrimers were prepared by the method described in the previous paper using the reaction of C_{60} with lithium acetylide connected to the dendron units in THF.[21] In the present study, *o*-dichlorobenzene (DCB) was used as a solvent for all spectroscopic measurements in order to compare with the data in the previous works. 1-Chloronaphthalene was employed for a viscous solvent. The electron donors such as *N*,*N*,*N*′,*N*′-tetramethyl-*p*-phenylenediamine (TMPD), *N*,*N*,*N*′,*N*′-tetramethylbenzidine (TMB), 1,4-diazabicyclo[2,2,2]octane (DABCO), and *N*,*N*-diethylaniline (DEA) were all commercially available reagents. β-Carotene and 1,8-diazabicyclo[5.4.0]undec-7-ene (DBU) were also commercial materials and used as received. Octyl viologen perchlorate (OV^{2+}) was prepared from commercially available chloride.

Apparatus. Nanosecond transient absorption spectra in the near-IR region (600−1200 nm) were measured using a second

* Corresponding authors.
[†] Kyoto University.
[‡] Tohoku University.

10.1021/jp0256995 CCC: $22.00
Published on Web 06/21/2002

SCHEME 1

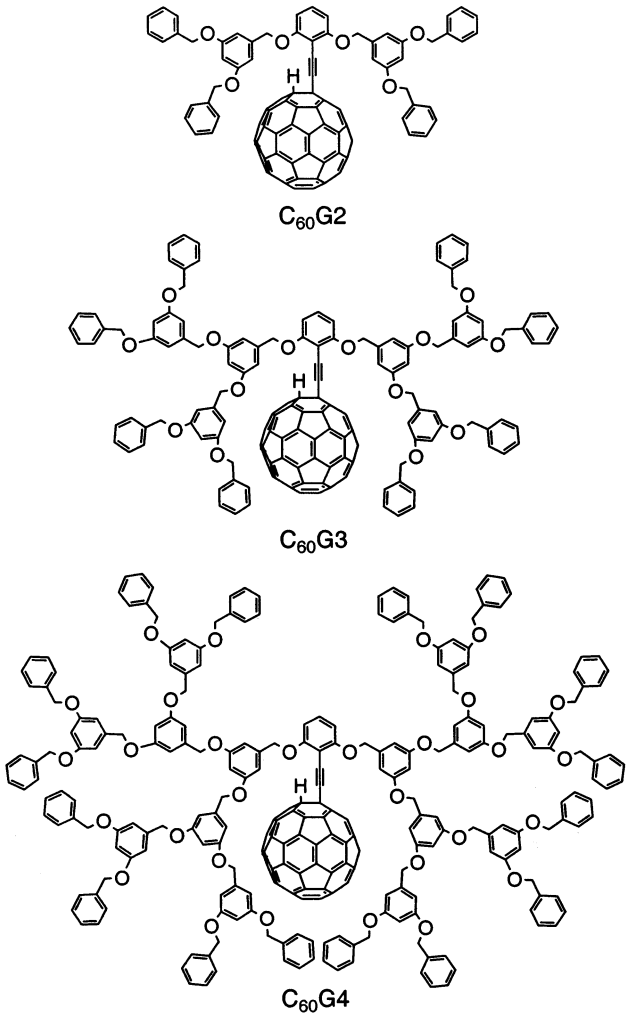

harmonic generation (SHG, 532 nm) of a Nd:YAG laser (Spectra-Physics, Quanta-Ray GCR-130, fwhm 6 ns, <20 mJ pulse^{-1}) as an excitation source. Monitoring light from a pulsed Xe-lamp was detected with a Ge-APD (Hamamatsu Photonics, B2834). For spectra in the visible region (400−1000 nm), a Si-PIN photodiode (Hamamatsu Photonics, S1722-02) was used as the detector. Triplet lifetime was estimated by using photomultiplier. Details of the transient absorption measurements were described in our previous paper.[22] All the samples were measured in a quartz cell (1 cm × 1 cm) and were deaerated by bubbling Ar through the solution for 15 min.

Steady-state fluorescence spectra in the visible region of the samples were measured on a Shimadzu RF-5300PC spectrofluorophotometer. Fluorescence spectra in the near-IR regions were detected by using an InGaAs detector.[23] Fluorescence lifetimes were measured by a single photon counting method using a streakscope (Hamamatsu Photonics, C4334-01). The samples were excited with SHG (410 nm) of a Ti:sapphire laser (Spectra-Physics, Tsunami 3950-L2S, fwhm 1.5 ps) equipped with a pulse selector (Spectra-Physics, 3980) and a harmonic generator (Spectra-Physics, GWU-23PS).

Steady-state absorption spectra in the visible and near-IR regions were measured with a JASCO V-570DS spectrometer at room temperature.

Oxidation and reduction potentials of the molecules in the present study were estimated in a conventional three-electrode cell controlled by a voltammetric analyzer (BAS CV-50W).

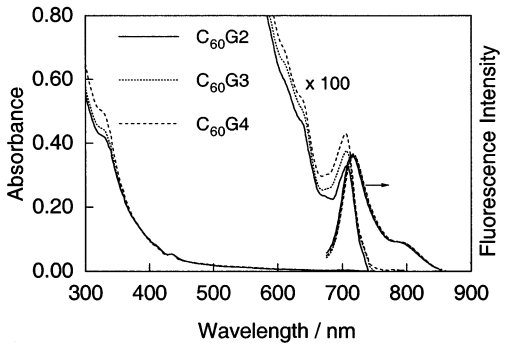

Figure 1. Steady-state absorption and fluorescence spectra of C_{60}G2, C_{60}G3, and C_{60}G4 in DCB (concentration ~10^{-5} M). In the fluorescence spectra, excitation wavelength was 400 nm and absorption intensities were matched at 400 nm.

TABLE 1: Properties of Photoexcited States of C_{60}G2, C_{60}G3, and C_{60}G4 in DCB

	C_{60}G2	C_{60}G3	C_{60}G4
excited singlet state			
λ_F/nm	715	717	717
τ_F/ns	1.36	1.37	1.34
Φ_F	1.2×10^{-3}	1.2×10^{-3}	1.2×10^{-3}
triplet state			
λ_{TT}/nm	690	700	700
τ_T/μs	38	38	37
k_{TT}/M^{-1} s^{-1}	5.6×10^8	3.3×10^8	1.4×10^8
Φ_{ISC}	0.83 ± 0.05	0.87 ± 0.05	0.81 ± 0.05

Results and Discussion

Steady-State Absorption and Fluorescence Spectra. The steady-state absorption spectra of C_{60}G2−C_{60}G4 showed absorption bands at 705 and 434 nm with a shoulder at 325 nm (Figure 1). These absorption bands are attributed to fullerene moieties of dendrimers: Positions of these absorption bands were similar to those of typical fullerene derivatives without dendron groups, such as methanofullerenes and so on.[24,25] The absorption bands due to the dendron groups appear in the wavelength region shorter than 320 nm. This finding indicates that the contribution of the excited states of the dendron groups is rather small in the present laser experiments, which were carried out with the visible lasers mainly.

Upon excitation with 400 nm light, these fullerene dendrimers in DCB showed fluorescence band at 715 nm with a shoulder around 785 nm. The fluorescence bands were generated from the fullerene moiety, since the 400 nm light excites only the fullerene moiety. The quantum yields for fluorescence were estimated as listed in Table 1 by using C_{60} as a standard (3.2×10^{-4}).[26] The quantum yields were the same for these fullerene dendrimers (1.2×10^{-3}). Increase in fluorescence quantum yields of fullerodendrimers more than pristine C_{60} can be attributed to the reduction of symmetry in the fullerene moiety.[25] The fluorescence lifetimes of the fullerene dendrimers were estimated to be 1.36, 1.37, and 1.34 ns for C_{60}G2, C_{60}G3, and C_{60}G4, respectively: These values are essentially identical within experimental error. Furthermore, the estimated lifetimes are almost the same as those reported for other mono-functional fullerene derivatives and pristine C_{60}.[25,27] These findings suggest that the dendron groups do not affect dynamic character of the lowest excited singlet state of the fullerene moiety.

Triplet Excited States. Upon the excitation of C_{60} dendrimers with the nanosecond laser light at 532 nm, a transient absorption spectrum was observed as shown in Figure 2 for C_{60}G2 as a representative case. The absorption band centered at 690 nm was attributed to the triplet state of the fullerene moiety, since

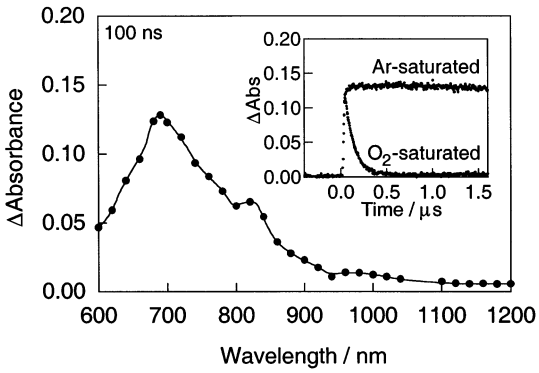

Figure 2. Transient absorption spectrum of $C_{60}G2$ (0.1 mM) in DCB at 100 ns after the 532 nm-laser irradiation. Inset: Absorption−time profiles at 690 nm in Ar- and O_2-saturated DCB.

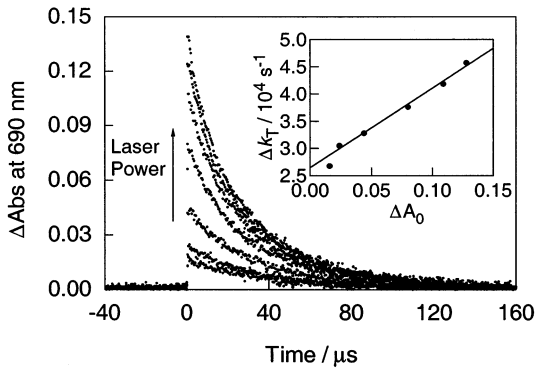

Figure 3. Absorption−time profiles at 690 nm of $C_{60}G2$ in DCB at various excitation laser power. Inset: Relation between Δk_T and ΔA_0.

the absorption bands decayed quickly in the presence of oxygen, which is an effective triplet energy acceptor (inset of Figure 2). The spectral shape of the transient absorption was only slightly changed with the change in the dendrimer generation.

The decay rates of the triplet states were strongly affected by the laser power as shown in Figure 3 for $C_{60}G2$ as a representative case. The decay time profiles are composed of mixed-order kinetics of first- and second-order, in which the former is the intrinsic decay rate of the triplet state and the latter is due to the triplet−triplet annihilation process (eq 1):

$$^3C_{60}{*}Gn + {}^3C_{60}{*}Gn \xrightarrow{k_{TT}} {}^1C_{60}{*}Gn + C_{60}Gn \qquad (1)$$

where $n = 1, 2, 3$.

The rate constants of first- and second-order kinetics were separately evaluated using the following equation (eq 2):

$$-\mathrm{d}[\ln(\Delta A_0)]/\mathrm{d}t = \Delta k_T = k_T{}^0 + (2k_{TT}/\epsilon_T)\Delta A_0 \qquad (2)$$

where ΔA_0, $k_T{}^0$, and ϵ_T are a T−T absorbance at $t = 0$, an intrinsic first-order decay rate of the triplet excited state of fullerene dendrimers, and an extinction coefficient of the triplet absorption band, respectively. As shown in an inset of Figure 3, plot of Δk_T to ΔA_0 shows a linear correlation. From the slope and the estimated ϵ_T value, the k_{TT} value was evaluated to be 5.6×10^8 M^{-1} s^{-1} for $C_{60}G2$ in DCB, which is one-order smaller than the diffusion-limiting rate of the solvent ($k_{diff} = 5.0 \times 10^9$ M^{-1} s^{-1} for DCB).[28] It is interesting to note that the k_{TT} values of $C_{60}G3$ and $C_{60}G4$ were estimated to be 3.3×10^8 and 1.4×10^8 M^{-1} s^{-1}, respectively. Thus, the k_{TT} value becomes small with an increase of the dendrimer generation. A similar trend was observed in more viscous solvents such as 1-chloronaphthalene; the k_{TT} values were estimated to be 4.8×10^8, 4.8×10^8, and 1.1×10^8 M^{-1} s^{-1} for $C_{60}G2$, $C_{60}G3$, and $C_{60}G4$, respectively. The smaller k_{TT} values observed for larger fullerodendrimers indicate that larger dendron groups disturb the triplet−triplet annihilation processes more effectively.

TABLE 2: Energy Transfer Rate Constants (M^{-1} s^{-1}) of $C_{60}G2$, $C_{60}G3$, and $C_{60}G4$ in DCB

quencher	$C_{60}G2$	$C_{60}G3$	$C_{60}G4$
O_2	1.3×10^9	1.2×10^9	8.5×10^8
β-carotene	1.4×10^9	3.3×10^8	3.2×10^8

The $k_T{}^0$ values were found to be 2.6×10^4, 2.6×10^4, and 2.7×10^4 s^{-1} for $C_{60}G2$, $C_{60}G3$, and $C_{60}G4$, respectively. Thus, the $k_T{}^0$ values are essentially the same, indicating no effect of the size of the dendron groups on the triplet lifetime, 37 or 38 μs (Table 1).

Energy Transfer Process of Fullerene Dendrimers. The absorption bands of the triplet excited states of the dendrimers were quenched in the presence of triplet energy quenchers such as molecular oxygen and β-carotene.

In the case of the energy transfer process with molecular oxygen, energy transfers from the triplet excited states of the fullerene dendrimers generate the singlet oxygen (eq 3):

$$^3C_{60}{*}Gn + {}^3O_2 \xrightarrow{k_q(O_2)} C_{60}Gn + {}^1O_2{*} \qquad (3)$$

where $n = 2, 3, 4$. The bimolecular quenching rate constants in the energy transfer process (eq 3) were estimated as listed in Table 2. It should be pointed out that the $k_q(O_2)$ values show a tendency similar to that observed in the triplet−triplet annihilation process: Smaller $k_q(O_2)$ values for larger dendron groups is attributed to the inhibition of collision of the C_{60} moiety with O_2. The energy transfer process (eq 3) was also confirmed by the observation of the fluorescence band due to the singlet oxygen at 1265 nm upon laser excitation of fullerene dendrimer in oxygen-saturated DCB. From the fluorescence intensities of the singlet oxygen band relative to that via triplet excited C_{60},[29] the quantum yields of the intersystem crossing processes (Φ_{ISC}) of $C_{60}G2$, $C_{60}G3$, and $C_{60}G4$ were estimated to be 0.83, 0.87, and 0.81, respectively. The estimated values are identical within the experimental error (± 0.05). Slightly lower Φ_{ISC} values than that for pristine C_{60} have been reported for other mono-functionalized fullerene derivatives.[25] The present finding indicates that excited states of the fullerodendrimers deactivate mainly via the triplet excited states. Thus, a variety of photoinduced processes is expected for the triplet excited states of fullerodendrimers.

Energy transfer process was observed in the transient absorption spectroscopy more clearly when the solution contained β-carotene as a triplet energy acceptor. In the transient absorption spectra of the solution including dendrimer and β-carotene, the energy transfer process (eq 4):

$$^3C_{60}{*}Gn + \beta\text{-carotene} \xrightarrow{k_q(\beta\text{-carotene})} C_{60}Gn + {}^3\beta\text{-carotene}{*} \qquad (4)$$

where $n = 2, 3, 4$, was confirmed by the observation of the absorption of the triplet excited β-carotene at 540 nm together with a decay of the triplet excited fullerene dendrimer, which was generated by selective excitation with 532 nm laser light (Figure 4). From the relation between the quenching rate of the triplet and the concentration of β-carotene, the bimolecular quenching rate constants for the present energy transfer processes were estimated as listed in Table 2. It is interesting to

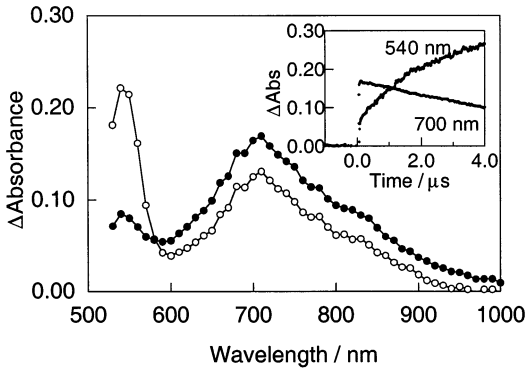

Figure 4. Transient absorption spectra of $C_{60}G4$ (0.1 mM) in DCB in the presence of β-carotene (0.1 mM) at 250 ns (filled circles) and 2.5 μs (open circles) after the laser irradiation. Inset: Absorption−time profiles at 700 and 540 nm.

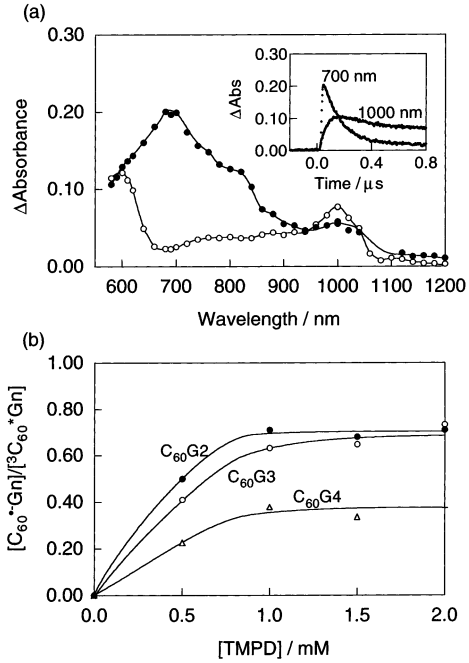

Figure 5. (a) Transient absorption spectra of $C_{60}G2$ (0.1 mM) in DCB in the presence of TMPD (2.0 mM) at 50 ns (filled circles) and 500 ns (open circles) after the laser irradiation. Inset: Absorption−time profiles at 1000 and 700 nm. (b) Relations between the $[C_{60}^{\bullet-}Gn]/[^3C_{60}{}^*Gn]$ values and the concentration of TMPD.

note that the ratio of the k_q(β-carotene) values of $C_{60}G2$ to that of $C_{60}G4$ was 4.5, while the ratios of rate constants of $C_{60}G2$ to $C_{60}G4$ for the triplet−triplet annihilation and the energy transfer to molecular oxygen were 4.0 and 1.5, respectively. This fact indicates that the ratio of the rate constants becomes smaller for molecules with smaller size due to easier penetration of smaller molecules closer to the fullerene core.

Photoinduced Electron-Transfer Processes. When the solution of the dendrimer contains an electron donor such as TMPD, photoinduced electron-transfer process is expected. Figure 5a is an example of the transient absorption spectra of a solution of the mixture of fullerene dendrimer ($C_{60}G2$) with TMPD. Immediately after the laser irradiation, an absorption band appeared at 700 nm, which is ascribed to the triplet excited state of $C_{60}G2$. At 500 ns after the laser irradiation, new absorption bands appeared at 620 and 1000 nm: The 620 nm band is assigned to the radical cation of TMPD,[30] while the 1000 nm band can be attributed to the radical anion of $C_{60}G2$; this absorption is located at the wavelength similar to those reported for the radical anion of mono-functionalized fullerene derivatives.[31,32] The generation of radical ions with the decrease in the triplet state absorption indicates that the photoinduced electron transfer occurred via the triplet excited state of $C_{60}Gn$ as shown in eq 5:

$$^3C_{60}{}^*Gn + \mathrm{TMPD} \xrightarrow{k_q(\mathrm{TMPD})} C_{60}^{\bullet-}Gn + \mathrm{TMPD}^{\bullet+} \quad (5)$$

where $n = 2, 3, 4$. Similar phenomena have been observed for $C_{60}G3$ and $C_{60}G4$.

From the relation between the triplet decay rate of $C_{60}G2$ and the concentration of TMPD, a bimolecular quenching rate constant (k_q(TMPD)) was estimated to be 3.7×10^9 M^{-1} s^{-1}. The efficiency of electron transfer can be calculated from the ratio of the maximal concentration of the generated radical ions to the initial concentration of the triplet states of fullerenes ($[C_{60}^{\bullet-}Gn]/[^3C_{60}{}^*Gn]$). For example, the $[C_{60}^{\bullet-}Gn]/[^3C_{60}{}^*Gn]$ values are plotted against the concentration of TMPD as shown in Figure 5b. The $[C_{60}^{\bullet-}Gn]/[^3C_{60}{}^*Gn]$ value is the function of concentration of donor as eq 6:

$$[C_{60}^{\bullet-}Gn]/[^3C_{60}{}^*Gn] = k_{ET}[\mathrm{donor}]/\{k_T + k_q[\mathrm{donor}]\} \quad (6)$$

where k_T and k_{ET} are decay rate of $^3C_{60}{}^*Gn$ in the absence of donor and electron-transfer rate constant, respectively. When $k_T \ll k_q$[donor], the $[C_{60}^{\bullet-}Gn]/[^3C_{60}{}^*Gn]$ value takes a constant value as shown in Figure 5b. Therefore, the constant value refers to the quantum yield (Φ_{ET}) via $^3C_{60}{}^*Gn$. Thus, the Φ_{ET} value of $C_{60}G2$ and TMPD was estimated to be 0.74 from Figure 5b. The k_{ET} value of the present electron-transfer process was estimated to be 2.7×10^9 M^{-1} s^{-1} from the relation of eq 6. Similar electron-transfer processes were observed with other fullerene dendrimers, $C_{60}G3$, $C_{60}G4$, with various electron donors. The parameters of the electron-transfer processes such as rate constants are summarized in Table 3.

As shown in Table 3, the Φ_{ET} values are in the order of $C_{60}G2 \approx C_{60}G3 > C_{60}G4$ for each donor, indicating that the shielding effect is effective for the fourth generation in the photoinduced electron-transfer processes. Furthermore, the k_{ET} values of the dendrimers become smaller in general for the dendrimers with increasing generation number, as observed in the previous sections for energy transfer processes. Especially, the change in the k_{ET} values is evident between the third and fourth generations: This is the same trend as reported for the shielding effects of the Fréchet-type dendrimers.[18] Furthermore, the k_{ET} values of the electron-transfer processes were in the order TMPD ≥ TMB > DABCO > DEA, which is in accord with the oxidation potentials of these donors.[33] These observations indicate that the dendron groups of the present fullerodendrimers act as a "barrier" rather than a "trap" for the donor molecules.[18] Thus, the observed k_q values of $^3C_{60}{}^*Gn$(k_q) can be explained on the basis of the free energy changes of the electron-transfer processes estimated by the Rehm−Weller relation.[34] The larger k_q values were observed for the reaction systems with sufficiently negative free energy changes. In Figure 6, the k_q values were plotted against ($E_{ox}-E_{red}-E_T$) values for the electron-transfer processes, which correspond to free energy changes without Coulombic term: E_{ox}, E_{red}, and E_T refer to oxidation potentials of aromatic amines, reduction potentials of fullerodendrimers, and triplet-state energy of fullerodendrimers, respectively. In Figure 6, lines were estimated from semiempirical Rehm−Weller relation by changing the distance of the encounter complex. As seen in Figure 6, the line assuming 7 Å for encounter distance does not fit well, although 7 Å is often

TABLE 3: Quenching Rate Constants, Quantum Yields, Electron Transfer Rate Constants, and Back Electron Transfer Rate Constants of the Electron Transfer Processes of the Dendrimers and Aromatic Amines

fullerene	donor	k_q[a]	Φ_{ET}	k_{ET}[a]	k_{BET}^{1st}[b]	k_{BET}^{2nd}[a]
C_{60}G2	TMPD	3.7×10^9	0.74	2.7×10^9	4.1×10^4	
	TMB	2.4×10^9	0.90	2.2×10^9		2.6×10^{10}
	DABCO	6.3×10^8	0.20	1.3×10^8	3.7×10^5	
	DEA	2.6×10^5	<0.1	$<10^5$		
C_{60}G3	TMPD	3.3×10^9	0.72	2.4×10^9		4.6×10^{10}
	TMB	1.8×10^9	0.93	1.7×10^9		2.5×10^{10}
	DABCO	4.8×10^8	0.23	1.1×10^8	4.4×10^5	
	DEA	2.3×10^5	<0.1	$<10^5$		
C_{60}G4	TMPD	1.6×10^9	0.38	6.1×10^8		4.2×10^{10}
	TMB	1.3×10^9	0.72	9.4×10^8		2.2×10^{10}
	DABCO	3.7×10^8	0.17	6.3×10^7	3.1×10^5	
	DEA	2.1×10^5	<0.1	$<10^5$		

[a] In M^{-1} s^{-1}. [b] In s^{-1}.

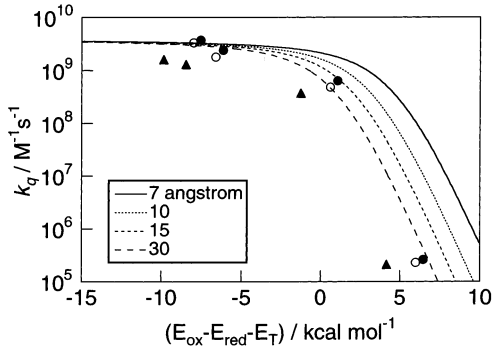

Figure 6. Relation between ($E_{ox}-E_{red}-E_T$) values and k_q of C_{60}G2 (filled circles), C_{60}G3 (open circles), and C_{60}G4 (filled triangles). Lines were estimated from Rehm−Weller relation assuming encounter distance is 7, 10, 15, and 30 Å.

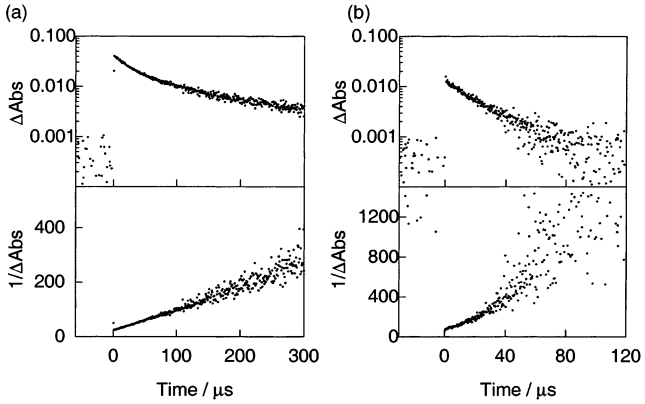

Figure 7. First- and second-order plots of absorption−time profiles of C_{60}G2 at 1000 nm in the presence of (a) TMB and (b) TMPD.

employed as an encounter distance of the electron-transfer systems of small molecules.[34] Better fit was observed by assuming a larger encounter distance such as 15 or 30 Å. This fact indicates that the electron transfer should occur at the longer distance due to the steric hindrance caused by the dendron groups.

Back Electron Transfer. The transient absorption bands due to the radical ions showed slow decay after reaching maximal concentrations. The decay of the radical ions can be attributed to the back electron-transfer processes. In the case of the radical ions generated in the electron-transfer system composed of C_{60}G2 and TMB, the decay of the radical ions obeyed second-order kinetics (Figure 7a), indicating that the radical ions are solvated as free ions (eq 7):

$$C_{60}^{\bullet-}Gn + \text{donor}^{\bullet+} \xrightarrow{k_{BET}^{2nd}} C_{60}Gn + \text{donor} \qquad (7)$$

where $n = 2, 3, 4$. On the other hand, in the case of the radical ions generated in the system of C_{60}G2 and TMPD, the decay obeyed first-order kinetics (Figure 7b), indicating that the radical ions were present as ion pairs (eq 8):[35,36]

$$(C_{60}^{\bullet-}Gn\cdots\text{donor}^{\bullet+})_{\text{ion pair}} \xrightarrow{k_{BET}^{1st}} C_{60}Gn + \text{donor} \qquad (8)$$

where $n = 2, 3, 4$.

The rate constants of back electron-transfer processes are also listed in Table 3. For all fullerene dendrimers, bimolecular kinetics (eq 7) was observed in the reaction systems using TMB as a donor, while in the systems with DABCO monomolecular kinetics (eq 8) was observed. It is interesting to note that, in the systems with TMPD, C_{60}G3 and C_{60}G4 obeyed a second-order kinetics while C_{60}G2 obeyed first-order kinetics. It should be pointed out that back electron-transfer process of pristine C_{60} obeyed first-order kinetics with all aromatic amines investigated in the present study in DCB. The observation of first-order kinetics with pristine C_{60} can be attributed to low stabilization energy of the solvation of each radical ion because of low dielectric constant of the solvent, DCB (dielectric constant = 9.93).[28] In the cases of the electron transfer systems of fullerene dendrimers and DABCO, first-order kinetics were observed presumably because a molecule of DABCO can penetrate into the dendron groups to reach the fullerene core due to its smaller size. On the other hand, TMB does not seem to be able to come close to the fullerene core due to its larger size, resulting in the outer-sphere electron transfer. Thus, the solvation as free ions is quite possible because of the lower Columbic interaction due to a longer distance. In the case of TMPD with intermediate size, the steric hindrance of dendron groups seems to be effective for the dendron groups larger than C_{60}G3.

Anions of Fullerene Dendrimers. In the above sections, dendron groups were shown to act as inhibitors in various photoinduced processes. This character of the dendron groups is considered to be useful to maintain chemically unstable species alive for a long period. In the present study, dynamic properties of chemically generated anions of fullerodendrimers were investigated. The anions of the fullerodendrimers ($C_{60}^{-}Gn$) were generated by using DBU according to Scheme 2.

The generations of the anions were confirmed by the steady-state absorption spectra: The anion of fullerodendrimer C_{60}G3 as a representative exhibited the absorption bands at 1584, 1282, 971, and 636 nm as shown in Figure 8. The anions were sensitive to molecular oxygen: The absorption bands of the anions gradually disappeared in the presence of oxygen. In the

SCHEME 2

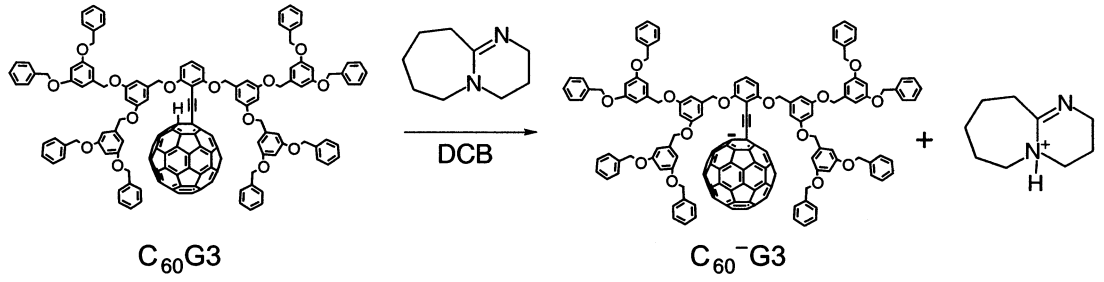

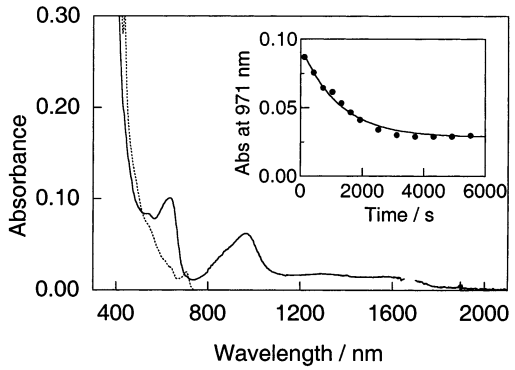

Figure 8. Steady-state absorption spectra of C_{60}G3 (0.1 mM) in DCB in the presence (solid line) and in the absence (dot line) of DBU (3.0 mM). Inset: Absorption−time profile at 971 nm in air-saturated DCB.

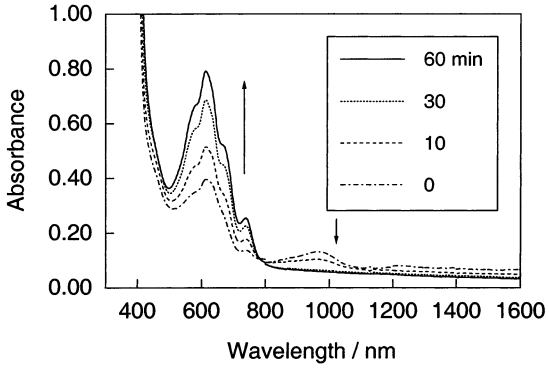

Figure 9. Steady-state absorption spectra of C_{60}G4 (0.1 mM) in DCB in the presence DBU (2.0 mM) and OV^{2+} (0.5 mM).

case of air-saturated solution, absorption bands disappeared over several minutes as shown in the inserted absorption−time profile in Figure 8. The spectral change in the air-saturated solution can be attributed to the electron transfer from C_{60}^{-}G*n* to molecular oxygen (eq 9):

$$C_{60}^{-}Gn + O_2 \rightarrow C_{60}^{\bullet}Gn + O_2^{\bullet-} \qquad (9)$$

where $n = 2, 3, 4$. In air-saturated solution, decay rate constants of anions of C_{60}G2, C_{60}G3, and C_{60}G4 were evaluated to be 8.8×10^{-1}, 4.6×10^{-1}, and 3.4×10^{-1} M^{-1} s^{-1}, respectively. The results indicate that the steric hindrance of larger dendron groups is also effective to protect the unstable species such as anions: The anion of C_{60}G4 can be kept alive for longer time than that of C_{60}G2 by a factor of 2.6. With the decrease in the anion, decomposition and dimerization of the fullerodendrimer radical were observed. The latter part of the absorption−time profile (inset of Figure 8) can be attributed to the generation of an absorption band due to the product(s) of these reactions.

The electron-transfer process from the anions to an electron acceptor was also confirmed in the reaction system containing octyl viologen (OV^{2+}). In the presence of OV^{2+}, new absorption bands appeared at 739, 614, and 404 nm, which are ascribed to the radical cation of octyl viologen ($OV^{\bullet+}$), with a concomitant decay of absorption bands of the anion (Figure 9). Appearance of absorption bands of $OV^{\cdot+}$ is apparently attributed to electron transfer from C_{60}^{-}G*n* to OV^{2+} (eq 10):

$$C_{60}^{-}Gn + OV^{2+} \rightarrow C_{60}^{\bullet}Gn + OV^{\bullet+} \qquad (10)$$

where $n = 2, 3, 4$.

It is notable that the generation rate of $OV^{\bullet+}$ becomes slower in the reaction with the fullerene anion with larger dendron groups: The bimolecular rate constants of eq 10 were estimated to be 1.0, 2.0×10^{-1}, and 1.6×10^{-1} M^{-1} s^{-1} for C_{60}G2, C_{60}G3, and C_{60}G4, respectively, indicating the steric hindrance to the electron transfer process by the dendron groups. Thus, the results prove that the reactive species such as anions can be kinetically stabilized by a larger dendron group: In the present case, the anion of C_{60}G4 has longer lifetime than C_{60}G2 by a factor of 6.3, which is larger than the factor observed in the reaction with O_2. This finding indicates that the dendrimer moiety protects the anion from the attack by a larger acceptor (OV^{2+}) more effectively than smaller one (O_2). From the comparison of absorption intensities of the generated $OV^{\bullet+}$ and decayed C_{60}^{-}G4, an extinction coefficient of C_{60}^{-}G4 at 971 nm was estimated to be 2.5×10^3 M^{-1} cm^{-1}. The extinction coefficients for other dendrimers were found to be essentially the same as that of C_{60}^{-}G4 independent of the dendrimer generation.

Conclusion

We have clarified the photophysical and photochemical properties of fullerene dendrimers having the dendrons from the second to fourth generation. The photophysical properties such as lifetimes of the singlet and triplet excited states of dendrimers were almost independent of the dendrimer generation. It was revealed that the dendron groups could control the rates of the various bimolecular reactions such as energy transfer and electron transfer processes of the fullerene core: Slow bimolecular processes were observed for the fullerenes with larger dendron groups. Also in the case of the back electron transfer process, the kinetics was also changed by the size of the dendron groups in addition to the size of donor radical cation. These dendron groups are also useful to kinetically stabilize the reactive species such as fullerene anions, which are produced chemically. The lifetimes of anions change according to the size of the dendron groups. Thus, the introduction of the dendron groups to the functional molecule such as fullerene was found to be a useful strategy to control its functions induced by the bimolecular processes.

Acknowledgment. The present work was partly supported by a Grant-in-Aid on Scientific Research from the Ministry of

Education, Culture, Sports, Science, and Technology of Japan (No. 12875163). The authors are also grateful for financial support by Core Research for Evolutional Science and Technology (CREST) of Japan Science and Technology Corporation. One of the authors (M.F.) thanks the Ogasawara Foundation for the Promotion of Science & Engineering for financial support.

References and Notes

(1) For review, see *Fullerenes*; Kadish, K. M., Ruoff, R. S., Eds.; Wiley-Interscience: New York, 2000.
(2) Nierengarten, J.-F. *Chem. Eur. J.* **2000**, *6*, 3667.
(3) Wooley, K. L.; Hawker, C. J.; Fréchet, M. J.; Wudl, F.; Srdanov, G.; Shi, S.; Li, C.; Kao, M. *J. Am. Chem. Soc.* **1993**, *114*, 9836.
(4) Hawker, C. J.; Wooley, K. L.; Fréchet, M. J. *J. Chem. Soc., Chem. Commun.* **1994**, 925.
(5) Cloutet, E.; Gnanou, Y.; Fillaut, J.-L.; Astruc, D. *Chem. Commun.* **1996**, 1565.
(6) Catalano, V. J.; Parodi, N. *Inorg. Chem.* **1997**, *36*, 537.
(7) Armaroli, N.; Boudon, C.; Felder, D.; Gisselbrecht, J.-P.; Gross, M.; Marconi, G.; Nicoud, J.-F.; Nierengarten, J.-F.; Vicinelli, V. *Angew. Chem., Int. Ed.* **1999**, *38*, 3730.
(8) Felder, D.; Gallani, J.-L.; Guillon, D.; Henrich, B.; Nicoud, J.-F.; Nierengarten, J.-F. *Angew. Chem., Int. Ed.* **2000**, *39*, 201.
(9) Brettreich, M.; Burghardt, S.; Böttcher, C.; Bayerl, T.; Bayerl, S.; Hirsch, A. *Angew. Chem., Int. Ed.* **2000**, *39*, 1845.
(10) Rio, Y.; Nicoud, J.-F.; Rehspringer, J.-L.; Nierengarten, J.-F. *Tetrahedron Lett.* **2000**, *41*, 10207.
(11) Schwell, M.; Wachter, N. K.; Rice, J. H.; Galaup, J.-P.; Leach, S.; Taylor, R. Bensasson, R. V. *Chem. Phys. Lett.*, **2001**, *339*, 29.
(12) Segura, J. L.; Gòmez, R.; Martín, N.; Luo, C.; Swartz, A.; Guldi, D. M. *Chem. Commun.* **2001**, 707.
(13) Accorsi, G.; Armaroli, N.; Eckert, J.-F.; Nierengarten, J.-F. *Tetrahedron Lett.* **2002**, *43*, 65.
(14) Takaguchi, Y.; Tajima, T.; Ohta, K.; Motoyoshiya, J.; Aoyama, H.; Wakahara, T.; Akasaka, T.; Fujitsuka, M.; Ito, O. *Angew. Chem., Int. Ed.* **2002**, *41*, 817.
(15) Nierengarten, J.-F.; Oswald, L.; Eckert, J.-F.; Nicoud, J.-F.; Armaroli, N. *Tetrahedron Lett.* **1999**, *40*, 5681.
(16) Numata, M.; Ikeda, A.; Fukuhara, C.; Sinkai, S. *Tetrahedron Lett.* **1999**, *40*, 6945.
(17) Eckert, J.-F.; Bryne, D.; Nicoud, J.-F.; Oswald, L.; Nierengarten, J.-F.; Numata, M.; Ikeda, A.; Shinkai, S.; Armaroli, N. *New J. Chem.* **2000**, *24*, 749.
(18) Hecht, S.; Fréchet, M. J. *Angew. Chem., Int. Ed.* **2001**, *40*, 74.
(19) Fujitsuka, M.; Kasai, H.; Masuhara, A.; Okada, S.; Oikawa, H.; Nakanishi, H.; Watanabe, A.; Ito, O. *Chem. Lett.* **1997**, 1211.
(20) Fujitsuka, M.; Kasai, H.; Masuhara, A.; Okada, S.; Oikawa, H.; Nakanishi, H.; Ito, O.; Yase, K. *J. Photochem. Photobiol. A* **2000**, *133*, 45.
(21) Murata, Y.; Ito, M.; Komatsu, K. *J. Mater. Chem.* **2002**, *12*, 2009.
(22) Fujitsuka, M.; Ito, O.; Yamashiro, T.; Aso, Y.; Otsubo, T. *J. Phys. Chem. A* **2000**, *104*, 4876.
(23) Fujitsuka, M.; Takahashi, H.; Kudo, T.; Tohji, K.; Kasuya, A.; Ito, O, *J. Phys. Chem. A* **2001**, *105*, 675.
(24) Eiermann, M.; Wudl, F.; Prato, M.; Maggini, M. *J. Am. Chem. Soc.* **1994**, *116*, 8364.
(25) Luo, C.; Fujitsuka, M.; Watanabe, A.; Ito, O.; Gan, L.; Huang, Y.; Huang, C.-H. *J. Chem. Soc., Faraday Trans.* **1998**, *94*, 527.
(26) Ma, B.; Sun, Y.-P. *J. Chem. Soc., Perkin Trans.* **1996**, 2157.
(27) Kim, D.; Lee, M.; Suh, Y. D.; Kim, S. K. *J. Am. Chem. Soc.* **1992**, *114*, 4429.
(28) Murov, S. L.; Carmichael, I.; Hug, G. L. *Handbook of Photochemistry*, 2nd ed.; Marcel Dekker: New York, 1993.
(29) Arbogast, J. W.; Darmanyan, A. P.; Foote, C. S.; Rubin, Y.; Diederich, F. N.; Alvarez, M. M.; Anz, S. J.; Whetten, R. L. *J. Phys. Chem.* **1991**, *95*, 11.
(30) Hausser, K. H.; Murrell, J. N. *J. Chem. Phys.* **1957**, *27*, 500.
(31) Guldi, D. M.; Hungerbuhler, H.; Asumus, K.-D. *J. Phys. Chem.* **1995**, *99*, 9380.
(32) Luo, C.; Fujitsuka, M.; Huang, C.-H.; Ito, O. *Phys. Chem. Chem. Phys.* **1999**, *1*, 2923.
(33) Kavarnos, G. J.; Turro, N. J. *Chem. Rev.* **1986**, *86*, 401.
(34) Rehm, D.; Weller, A. *Isr. J. Chem.* **1970**, *8*, 259.
(35) Ito, O.; Sasaki, Y.; Yoshikawa, Y.; Watanabe, A. *J. Phys. Chem.* **1995**, *99*, 9838.
(36) Fujitsuka, M.; Luo, C.; Ito, O. *J. Phys. Chem. B* **1999**, *103*, 334.